POLITECNICO DI TORINO
Repository ISTITUZIONALE

Rectangular Dielectric Resonator Antenna with Corrugated Walls

Original
Rectangular Dielectric Resonator Antenna with Corrugated Walls / Fakhte, Saeed; Matekovits, Ladislau; Aryanian, Iman. - In: IEEE ACCESS. - ISSN 2169-3536. - ELETTRONICO. - 7:(2019), pp. 3422-3429. [10.1109/ACCESS.2018.2888555]

Availability:
This version is available at: 11583/2723142 since: 2019-01-17T10:12:21Z

Publisher:
IEEE

Published
DOI:10.1109/ACCESS.2018.2888555

Terms of use:

This article is made available under terms and conditions as specified in the corresponding bibliographic description in the repository

Publisher copyright
IEEE postprint/Author's Accepted Manuscript

©2019 IEEE. Personal use of this material is permitted. Permission from IEEE must be obtained for all other uses, in any current or future media, including reprinting/republishing this material for advertising or promotional purposes, creating new collecting works, for resale or lists, or reuse of any copyrighted component of this work in other works.

(Article begins on next page)

12 October 2024

IEEE Access
Multidisciplinary : Rapid Review : Open Access Journal

Received November 15, 2018, accepted December 13, 2018, date of publication December 25, 2018, date of current version January 11, 2019.

Digital Object Identifier 10.1109/ACCESS.2018.2888555

Rectangular Dielectric Resonator Antenna With Corrugated Walls

SAEED FAKHTE[1,2], LADISLAU MATEKOVITS[2,3], (Senior Member, IEEE), AND IMAN ARYANIAN[1]

[1]Iran Telecommunication Research Center, Tehran 14155-3961, Iran
[2]Department of Electronics and Telecommunications, Politecnico di Torino, 10129 Turin, Italy
[3]School of Engineering, Macquarie University, Sydney, NSW 2109, Australia

Corresponding author: Ladislau Matekovits (ladislau.matekovits@polito.it)

This work was supported in part by the Iran Telecommunication Research Center, Tehran, Iran, and in part by the project "Advanced Nonradiating Architectures Scattering Tenuously and Sustaining Invisible Anapoles," funded by the Compagnia di San Paolo in the framework of joint projects for the Internationalization of Research–2017.

ABSTRACT A wideband and high-gain rectangular dielectric resonator antenna (RDRA) with corrugated walls is introduced. By generating corrugation in two opposite sidewalls of the RDRA, the radiation intensity from them compared to that of the top wall increases, which in turn will raise the boresight gain of the antenna. Also, the presence of the higher air content in the antenna body lowers the effective dielectric constant of the RDRA, leading to a wideband configuration. For demonstration, the proposed antenna is designed, fabricated, and measured. The measured results show that the proposed antenna radiates in the broadside direction with a high gain of 9 dB. Also, a wide impedance bandwidth of 15.3% from 3.57 to 4.16 GHz is achieved. In addition, the radiation efficiency of more than 90% over the whole bandwidth is attained. A good agreement between the simulated and measured results is attained.

INDEX TERMS Gain, fundamental mode, impedance bandwidth, rectangular dielectric resonator antenna (RDRA).

I. INTRODUCTION

Dielectric resonator antennas (DRAs) have received much attention due to several attractive characteristics such as light weight, low profile and high radiation efficiency [1]. Even though DRAs have originally been recognized for millimeter wave applications, they are also extensively studied at microwave frequency [2]–[4]. They are appropriate alternatives for compact antennas, such as microstrip antennas. DRAs avoid the intrinsic disadvantages of them, such as high conduction loss at millimeter-wave frequencies and low efficiency due to surface wave excitation [5], [6]. Moreover, in current microwave systems, the broadband antennas having appropriate gain and good radiation efficiency with compact structure, such as mobile and portable radio devices, are required.

The gain enhancement of DRAs without using an array of elements has been the subject of many investigations, e.g., [7]–[13]. Numerous techniques have been proposed to increase the boresight gain of a DRA, such as the use of electromagnetic bandgap structures (EBG) [7], a short horn around the DRA [8], a metallic patch as the superstrate [9], operation at a higher order mode [10], anisotropic material in the DRA prism [11], [12], and engraved grooves on the side walls [13]. Also, several approaches for bandwidth enhancement of the DRAs have been reported, such as merging two adjacent resonators [14], decreasing the effective permittivity of the DRA [15]–[20], and modifying the feed geometries [21].

The typical gain values for the RDRA operating at its lowest order mode is about 5 dB, when placed on a large ground plane [10]. Recently, it has been shown that by increasing the radiations from the sidewalls of a DRA operating at its fundamental radiating mode, its gain increases [11]–[13]. In [11], the use of uniaxial anisotropic material inside the RDRA increased the radiations from its sidewalls compared to that of the top wall due to the lowest order TE^{y}_{111} mode, which improved the antenna boresight gain. In [12], the use of uniaxial anisotropic material has been also proved to be very effective for enhancing the boresight gain of a cylindrical DRA operating at its fundamental radiating $HEM_{11\delta}$ mode. In [13], this increase of the radiation has been obtained by engraving two grooves in two opposite sidewalls of the dielectric prism. The radiation mechanism has been analyzed in [13], and will not be reported here.

2169-3536 © 2018 IEEE. Translations and content mining are permitted for academic research only.
Personal use is also permitted, but republication/redistribution requires IEEE permission.
See http://www.ieee.org/publications_standards/publications/rights/index.html for more information.

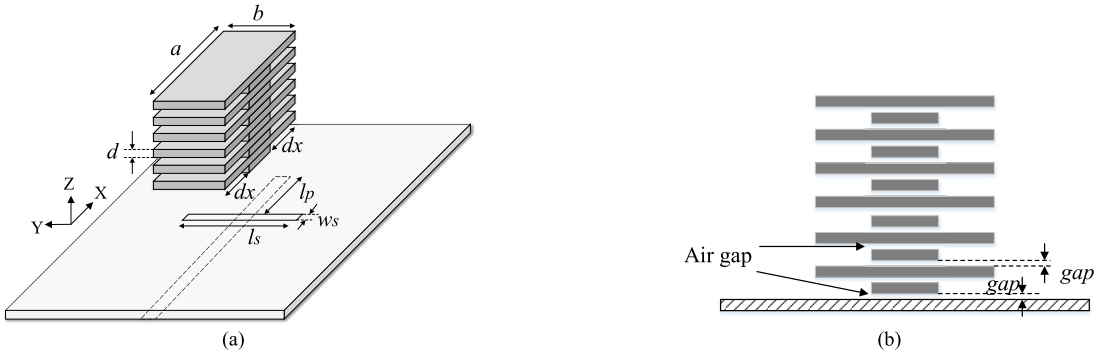

FIGURE 1. The configuration of the proposed DRA, (a) 3D view, (b) side view.

The same technique has been adopted in the present work, but instead of a single groove, a periodic sequence of such perturbations is considered. This distributed load gives rise to a similar to the corrugated structure on two out of four sidewalls of the RDRA, hence to a drastic change in the boundary conditions. So, for the first time, a RDRA with corrugated walls is investigated. It is shown that by generating corrugations over two opposite sidewalls of the RDRA, the radiation intensity from these faces compared to the top wall increases, which in turn enhances the boresight gain of the proposed antenna [11]–[13]. In addition, due to the presence of the air in the antenna structure, the effective permittivity of the DRA decreases, which determines an increase in the impedance bandwidth of the antenna.

The paper is organized as follows: In Section II, a brief discussion of the design procedure is provided. In Section III, the measured results of the proposed antenna are presented and compared with the simulated results. A good agreement between these results is attained. Finally, Section IV gives the conclusions.

II. ANTENNA CONFIGURATION

Figure 1 shows the antenna configuration. The proposed DRA is fabricated by placing 12 layers of Rogers TMM13i with the dielectric constant of $\varepsilon_r = 12.2$, loss tangent of $tan\delta = 0.0019$ and thickness of $d = 1.27$ mm onto each other. Note that the air gap between the layers and also between the bottom layer and the ground plane is inevitable. The effect of such an air gap is studied extensively in [22]–[24]. So, its effect on the antenna performance should be studied and quantified.

The DRA structure has been parametrized as follows: rectangular radiation aperture of edge-lengths a and b; corrugation depth dx. The antenna is fed through a slot of length l_s and width w_s positioned in a metallic ground plane. This later lays on a substrate of h = 0.508 mm and characterized by a relative dielectric constant $\varepsilon_r = 3.38$. On the opposite side of the dielectric, there is a microstrip line of width $w_{mstrip} = 1.15$ mm (that will guarantee a 50 Ω characteristic impedance). Input matching is achieved with an inductive stub with the length of l_p. Also, the ground plane size is 10×10 cm^2.

The initial dimensions of the antenna are obtained as follows: to account for the effect of the air gap on the resonant frequency of the proposed DRA, the dielectric waveguide model (DWM) [1] is improved by including an effective permittivity ε_{eff} [25], [26]. The DRA itself is modeled as a complete rectangular prism with the effective permittivity ε_{eff} calculated using the method reported in [25] and [26]. Finally, the antenna performances in terms of the reflection coefficient and gain are optimized. As a result of the optimization, the proposed antenna parameters result to be as follows: $a = 30$ mm, $b = 23$ mm, $dx = 10$ mm, $l_p = 14$ mm, $l_s = 34$ mm, $w_s = 1.5$ mm.

The calculated resonant frequency of the TE^y_{111} mode is 2.7 GHz. The resonant frequency is also obtained by the eigenmode solver of HFSS which does not consider the feed effects. The calculated resonant frequency of the HFSS eigenmode solver is 3.5 GHz. The discrepancy between the simulated and calculated resonant frequencies is mainly due to the irregular shape of the DRA, and to the fact that in the DWM method the overall DRA has been considered as made up of the effective dielectric constant, while this is valid only on part. Since the central part of the DRA exhibits a higher value of the dielectric constant $\varepsilon_r > \varepsilon_{eff}$, the resulting resonant frequency (computed by this model) is expected to be lower. However, even though the DWM method is not so accurate here, but is still useful for the prediction of the first guess of the resonant frequency.

To ensure that the fundamental mode is excited and the gain enhancement is not based on the well-known technique of higher-order modes [10], the proposed DRA is analyzed by the eigenmode solver in HFSS. The eigenmode solver gives resonant frequency and field distribution of all modes, which can be excited in the DRA (without explicitly considering the excitation). To analyze structures with open boundaries such as antennas in the eigenmode solver of HFSS, the structures should be surrounded by perfect matched layer (PML) boundary. PML is an artificial absorbing layer, used to truncate computational region. The eigenmode solver can also calculate the unloaded quality factor of the different

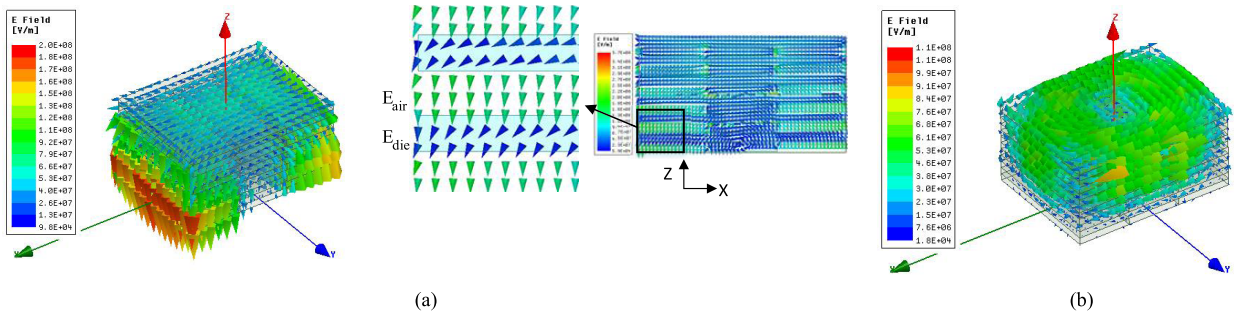

FIGURE 2. Simulated electric field distribution plots of isolated DRA residing on an infinite ground plane by eigenmode solver of Ansoft HFSS (a) TE^{y}_{111} mode at 3.5 GHz, (left) 3D view, (Right) Side view (b) $TE^{z}_{011+\delta}$ mode at 3.98 GHz.

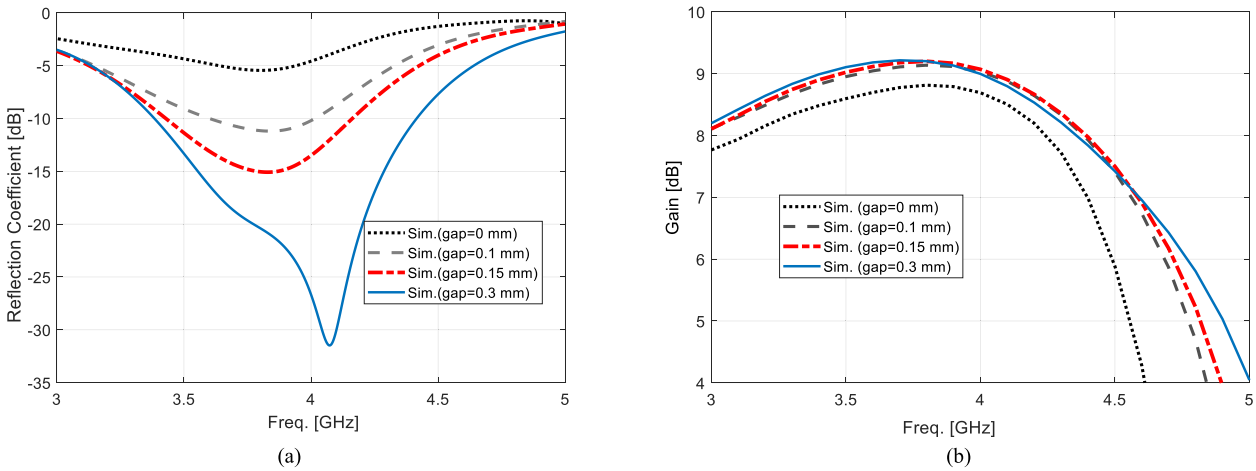

FIGURE 3. The simulated results for different values of the gap heights, (a) Reflection coefficient, (b) Boresight gain.

modes of the DRA. Because the use of ports and sources are not allowed in the eigenmode problems, the Q calculated does not contain losses due to those sources. Once the simulation is done in the HFSS, the type of the modes and the number of their indices can be identified from the E- and H- field distributions inside the DRA.

It is observed in Fig. 2 that there is no higher-order mode with broadside radiation within the frequency range 3.5-4.2 GHz. Fig. 2(a) shows the electric field distribution of TE^{y}_{111} mode. It is noted that the electric field intensity on the sidewalls of the DRA where the corrugations have been applied is much stronger than that of the top wall. Also, the electric field distribution in Fig. 2(b) is due to the $TE^{z}_{011+\delta}$ mode with non-broadside radiation pattern [3].

Observe in Fig. 2(a) that, the strength of the Ez component normal to the air-dielectric interface in the corrugation regions is increased to satisfy the continuity condition [13]. By enforcing the normal E field boundary condition across the interface between the dielectric parts of the DRA and the corrugations, a relation between the electric fields in both regions at the interface can be obtained.

$$E_{air} = \varepsilon_r E_{die} = 12.2 E_{die} \tag{1}$$

where E_{air} and E_{die} are the z-components of the electric fields inside the corrugation and the DRA, respectively. Also, $\varepsilon_r = 12.2$ is the dielectric constant of the DRA. As shown in equation (1) and Fig. 2(a), E_{air} is stronger than E_{die}. Note that the electric field inside the DRA at the top segment has nearly the same strength as that of the vicinity of the interface. Therefore, it can be expected that by increasing the corrugation depth, the strength of the electric field in the corrugations will increase because of the increase in the length of the interface between the DRA and the corrugations.

A parametric study is conducted to examine the effect of DRA dimensions on the antenna performance. In the study, only one parameter is varied at one time, i.e., without changing any other parameters. This study has been performed using CST Microwave Studio.

The reflection coefficient and gain of the antenna are computed for different values of the gap height g as shown in Fig. 3. The structure is simulated by considering the air gaps between the layers and also between the bottom layer and the ground plane. Observe in Fig. 3(a) that the air gap thickness substantially affects the input impedance of the antenna. So that, by increasing it, the reflection coefficient changes considerably. Also, by increasing the gap thickness from $gap = 0$ to $gap = 0.1$ mm, the antenna gain is

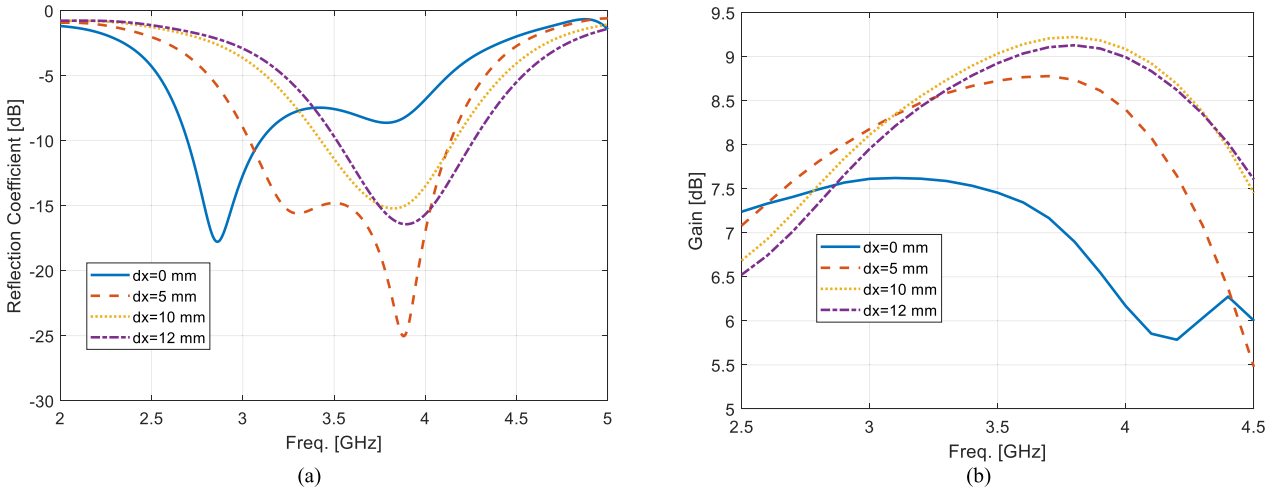

FIGURE 4. The simulated results for different values of the corrugation height, dx, (a) Reflection coefficient, (b) Boresight gain.

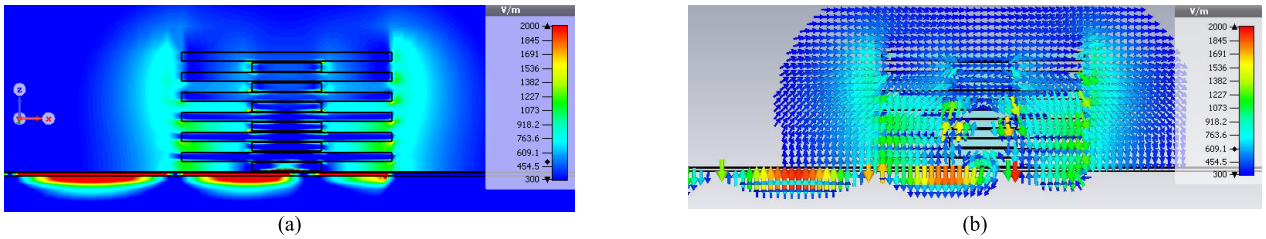

FIGURE 5. The E-field distribution of the proposed antenna at 3.7 GHz, (a) electric field amplitude plot, (b) electric field vector plot.

increased. This happens because the field intensity over the sidewalls increases. But, a further increase in the gap thickness, does not considerably change the boresight gain. Note that, the air gap thickness of $gap = 0.15$ mm is considered in the simulations in order to optimize the antenna performance. This value for the air gap is chosen based on the measurement results, so that by considering it a good agreement between the simulation and measurement results is attained. Different values of the air gap thickness between the bottom layer of the DRA and the ground plane [22]–[24] and also between the layers of the DRA [27] have been reported. It ranges from 0.02 mm to 0.152 mm.

Fig. 4 shows the variation of the reflection coefficient and gain along with the operating frequency with the change in corrugation height, dx. Observe in Fig. 4(a) that, there are two minima in the reflection coefficient curve. These two minima correspond to the TE^y_{111} mode of the DRA and to the slot. Note that, the lower minimum points of reflection coefficient curves move towards the lower frequencies for higher heights of corrugation (dx), whereas the upper are relatively stable. So, one can conclude that, the lower minima are related to the TE^y_{111} mode of the DRA and the upper ones are related to the slot. Also, observe in Fig. 4(b) that, increasing the corrugation height from $dx = 0$ to $dx = 10$ mm results in an increase in the peak gain from 7.6 dB to 9.1 dB as well as an upward shift in the frequency of maximum gain of the antenna. However, a further increase in dx will not considerably change the gain.

In [11] and [13], it has been shown that the far-field radiation patterns of the RDRA operating in the TE^y_{111} mode can be calculated by replacing it with equivalent magnetic surface current densities over the side and top walls. Then, it has been proven that the radiation pattern due to these current densities over the sidewalls of the RDRA is more directive than those flowing on the top wall in the boresight direction ($\theta = 0°$). Consequently, by increasing the radiation intensity from the sidewalls compared to the other walls of RDRA, its overall directivity in the boresight direction can be improved. On the other hand, considering the relation between the magnetic surface current density and tangential electric field relative to the interface of the dielectric and air, in order to increase the magnitude of the magnetic surface current density over the sidewalls the magnitude of the electric field should be increased.

Figure 5 shows the electric field distribution of the TE^y_{111} mode at 3.7 GHz obtained using CST MWS. Observe that, by increasing the height of corrugation, the magnitude of the z-component of the electric field at sidewalls is strengthened compared to that of x-component over the top wall of DRA. Thus, an increase in the directivity and gain of the antenna is expected.

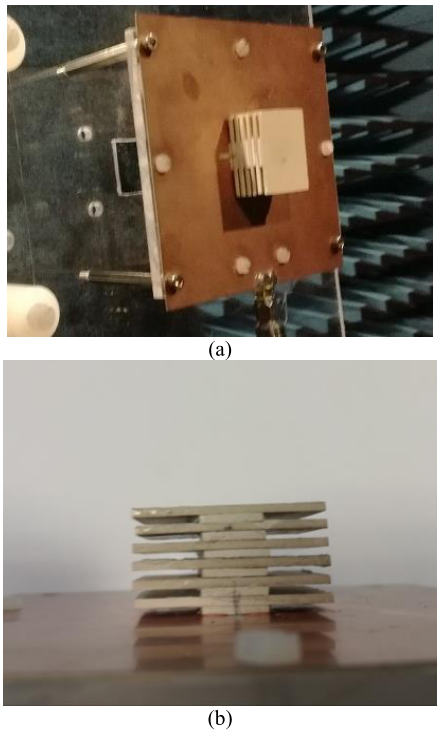

FIGURE 6. The fabricated prototype of the proposed antenna, (a) 3D view, (b) Side view.

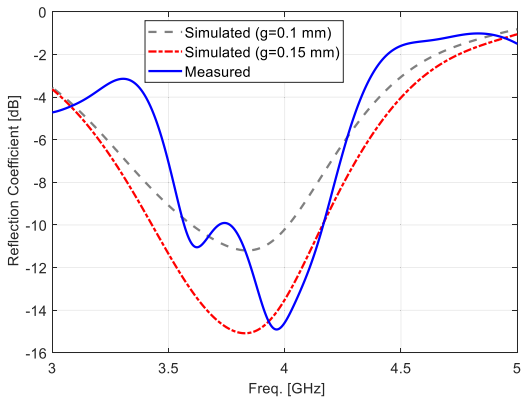

FIGURE 7. Measured and simulated reflection coefficients.

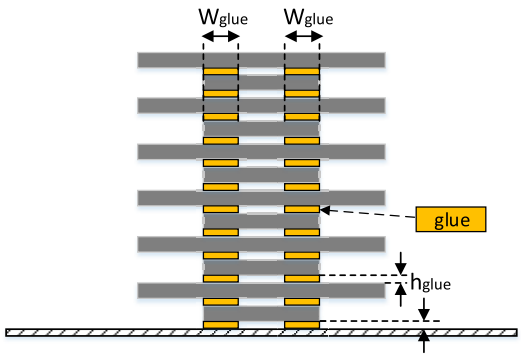

FIGURE 8. The side view of the proposed DRA. The glue layers are shown by yellow rectangles.

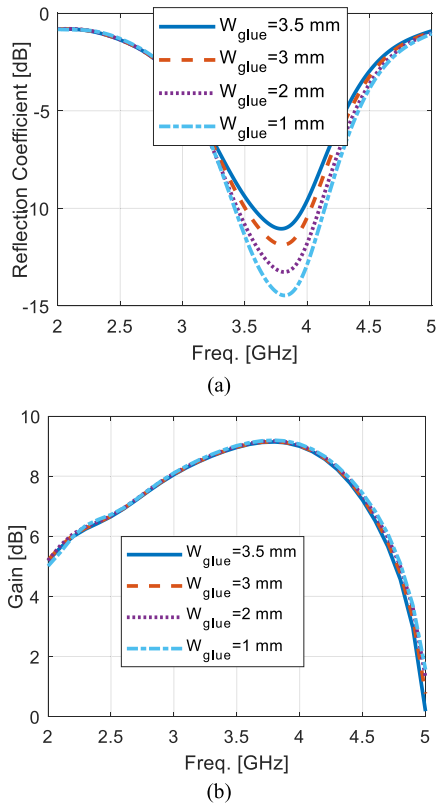

FIGURE 9. Simulated results of the corrugated DRA by considering the effect of the adhesive material width, W_{glue}, (a) reflection coefficient, (b) gain.

III. MEASURED RESULTS

A prototype of the proposed antenna is fabricated and tested, to validate the results of the simulation. Fig. 6(a) shows the prototype of the proposed antenna mounted on the test fixture in the anechoic chamber. Also, Fig. 6(b) shows the side view of the DRA. Note that, there are some misalignments between the layers, which are because of the fabrication difficulty of the proposed structure (many small pieces controlled by hand, that could also slide during the solidification process of the glue). The measured and simulated reflection coefficients are shown in Fig. 7. As previously mentioned, the existence of the air gaps between the dielectric layers is inevitable. So that, observe in Fig. 7 that, by considering the air gap thickness of $gap = 0.1$ mm or $gap = 0.15$ mm, the simulated results are in close agreement with the measured result. The measured impedance bandwidth is 15.3%, from 3.57 to 4.16 GHz. Note that, the impedance bandwidth enhancement is owing to the lowering of the effective permittivity of the antenna. The reflection coefficient level of this antenna is not very good but is still acceptable. Because the threshold value for the input reflection coefficient of the antennas is -10dB ($|s_{11}| < -10dB$). There are a lot of works on the DRAs in which the measured and simulated reflection coefficients vary between the values of -10dB and -15dB [28]–[32].

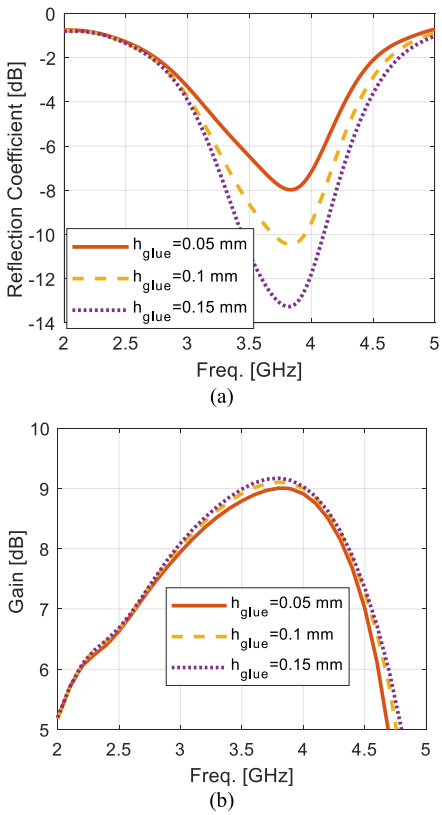

FIGURE 10. Simulated results of the corrugated DRA by considering the effect of the adhesive material height, gap (a) reflection coefficient, (b) gain.

To fix the dielectric layers onto each other and also the bottom layer on the ground plane, a commercially available adhesive material with the permittivity of $2.2 - j0.022$ is used [33]. As shown in Fig. 8, the glue is only applied in the vicinity of the sidewalls of the notched region. The width and height of the applied glue layers are denoted as W_{glue} and h_{glue}.

Fig. 9 shows the effect of the glue width on the reflection coefficient and boresight gain of the DRA. Note that the values of the other parameters of the antenna are as mentioned earlier. Also, the thickness of the glue is chosen to be $h_{glue} = 0.15mm$. However, observe that as the glue width is increased, the reflection coefficient worsens. On the other hand, decreasing the glue width leads to the fabrication complexity. Therefore, a tradeoff must be made between the impedance bandwidth and manufacturing difficulty. Thus, the width of the glue is considered to be $W_{glue} = 2mm$. Also, as shown in Fig. 9 (b), changing the glue width does not have considerable effect on the boresight gain of the antenna.

Fig. 10 depicts the change in the simulated reflection coefficient and boresight gain of the corrugated DRA with the variation of the glue thickness, h_{glue}. Observe in Fig. 10 (a) that decreasing the thickness of the glue layers worsens the impedance bandwidth of the antenna. So, the glue thickness is determined to be 0.15 mm. Also, observe in Fig. 10 (b) that, the boresight gain of the antenna is slightly affected by the glue thickness.

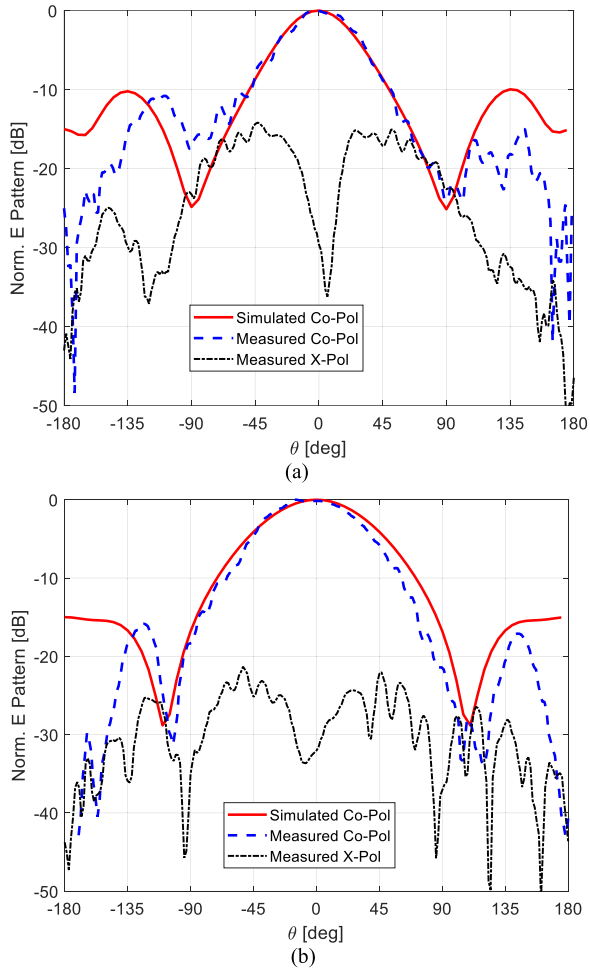

FIGURE 11. Measured and simulated radiation patterns at 3.87 GHz in (a) XZ plane, (b) YZ plane.

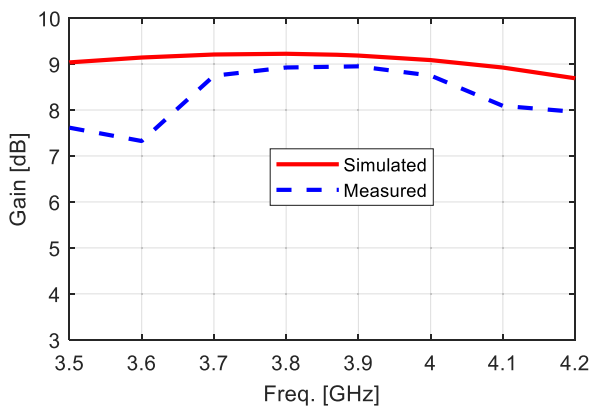

FIGURE 12. The measured and simulated antenna gain in the boresight direction versus frequency.

The normalized far field radiation pattern (dB) for antenna is presented in Figs. 11(a) and 11(b). Fig. 11(a) shows the E-field radiation pattern versus θ when φ is specified to be 0° (XZ plane). Also, Fig. 11(b) shows the E-field radiation

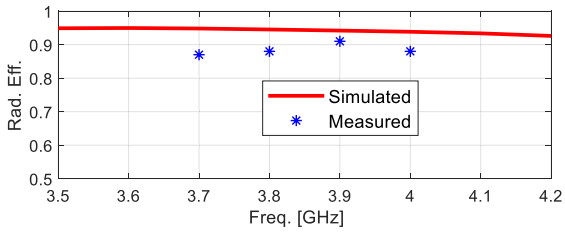

FIGURE 13. The radiation efficiency of the proposed antenna.

pattern versus θ when φ is specified to be 90° (YZ plane). The antenna radiates broadside in both XZ and YZ planes which is desirable for wireless applications. Also, the measured cross polarization level is 30 dB or more below the co-polarization level at boresight direction in both planes. The simulated and measured antenna gains are shown in Fig. 12. Observe that, a gain higher than 9 dB is obtained over the whole operation band, indicating that the aforementioned corrugation technique can be an efficient method for the gain enhancement. Moreover, the simulated radiation efficiency is more than 90%, as shown in Fig. 13. The measured results of the radiation efficiency also show a high efficiency of about 90%.

IV. CONCLUSION

A rectangular DRA with the corrugations on its sidewalls is proposed, which has a wide impedance bandwidth, improved gain and a high radiation efficiency. By generating the corrugations, the radiation intensity from the sidewalls of the DRA compared to that of the top wall increases, which in turn enhances the directivity of the antenna. A prototype has been fabricated and verified experimentally. The simulated and measured results are in a close agreement.

ACKNOWLEDGMENT

The authors would like to thank G. Dassano for his assistance in the fabrication and measurement of the antenna prototype model.

REFERENCES

[1] A. Petosa, *Dielectric Resonator Antenna Handbook*. Norwood, MA, USA: Artech House, 2007.

[2] A. Petosa and A. Ittipiboon, "Dielectric resonator antennas: A historical review and the current state of the art," *IEEE Antennas Propag. Mag.*, vol. 52, no. 5, pp. 91–116, Oct. 2010.

[3] R. K. Mongia and P. Bhartia, "Dielectric resonator antennas—A review and general design relations for resonant frequency and bandwidth," *Int. J. Microw. Millim.-Wave Comput.-Aided Eng.*, vol. 4, no. 3, pp. 230–247, 1994.

[4] K. W. Leung, E. H. Lim, and X. S. Fang, "Dielectric resonator antennas: From the basic to the aesthetic," *Proc. IEEE*, vol. 100, no. 7, pp. 2181–2193, Jul. 2012.

[5] S. Fakhte and H. Oraizi, "Compact uniaxial anisotropic dielectric resonator antenna operating at higher order radiating mode," *Electron. Lett.*, vol. 52, no. 19, pp. 1579–1580, Aug. 2016.

[6] A. Petosa, A. Ittipiboon, Y. M. M. Antar, D. Roscoe, and M. Cuhasi, "Recent advances in dielectric-resonator antenna technology," *IEEE Antennas Propag. Mag.*, vol. 40, no. 3, pp. 35–48, Jun. 1998.

[7] T. A. Denidni, Y. Coulibaly, and H. Boutayeb, "Hybrid dielectric resonator antenna with circular mushroom-like structure for gain improvement," *IEEE Trans. Antennas Propag.*, vol. 57, no. 4, pp. 1043–1049, Apr. 2009.

[8] N. Nasimuddin and K. P. Esselle, "A low-profile compact microwave antenna with high gain and wide bandwidth," *IEEE Trans. Antennas Propag.*, vol. 55, no. 6, pp. 1880–1883, Jun. 2007.

[9] S. Fakhte, H. Oraizi, and M. H. Vadjed-Samiei, "A high gain dielectric resonator loaded patch antenna," *Prog. Electromagn. Res. C*, vol. 30, pp. 147–158, Feb. 2012.

[10] A. Petosa and S. Thirakoune, "Rectangular dielectric resonator antennas with enhanced gain," *IEEE Trans. Antennas Propag.*, vol. 59, no. 4, pp. 1385–1389, Apr. 2011.

[11] S. Fakhte, H. Oraizi, and L. Matekovits, "High gain rectangular dielectric resonator antenna using uniaxial material at fundamental mode," *IEEE Trans. Antennas Propag.*, vol. 65, no. 1, pp. 342–347, Jan. 2017.

[12] S. Fakhte, H. Oraizi, L. Matekovits, and G. Dassano, "Cylindrical anisotropic dielectric resonator antenna with improved gain," *IEEE Trans. Antennas Propag.*, vol. 65, no. 3, pp. 1404–1409, Mar. 2017.

[13] S. Fakhte, H. Oraizi, and L. Matekovits, "Gain improvement of rectangular dielectric resonator antenna by engraving grooves on its side walls," *IEEE Antennas Wireless Propag. Lett.*, vol. 16, pp. 2167–2170, 2017.

[14] Z. Fan and Y. M. M. Antar, "Slot-coupled DR antenna for dual-frequency operation," *IEEE Trans. Antennas Propag.*, vol. 45, no. 2, pp. 306–308, Feb. 1997.

[15] D. Guha, Y. M. M. Antar, A. Ittipiboon, A. Petosa, and D. Lee, "Improved design guidelines for the ultra wideband monopole-dielectric resonator antenna," *IEEE Antennas Wireless Propag. Lett.*, vol. 5, pp. 373–376, 2006.

[16] K. S. Ryu and A. A. Kishk, "UWB dielectric resonator antenna having consistent omnidirectional pattern and low cross-polarization characteristics," *IEEE Trans. Antennas Propag.*, vol. 59, no. 4, pp. 1403–1408, Apr. 2011.

[17] M. Khalily, M. K. A. Rahim, and A. A. Kishk, "Bandwidth enhancement and radiation characteristics improvement of rectangular dielectric resonator antenna," *IEEE Antennas Wireless Propag. Lett.*, vol. 10, pp. 393–395, 2011.

[18] A. Al-Zoubi, F. Yang, and A. Kishk, "A broadband center-fed circular patch-ring antenna with a monopole like radiation pattern," *IEEE Trans. Antennas Propag.*, vol. 57, no. 3, pp. 789–792, Mar. 2009.

[19] R. Chair, A. A. Kishk, and K. F. Lee, "Wideband dual polarized dielectric resonator antennas at X-band," in *Proc. IEEE Antennas Propag. Soc. Int. Symp.*, vol. 4B, Jul. 2005, pp. 214–217.

[20] R. Chair, A. A. Kishk, and K. F. Lee, "Experimental investigation for wideband perforated dielectric resonator antenna," *Electron. Lett.*, vol. 42, no. 3, pp. 137–139, Feb. 2006.

[21] K. M. Luk, M. T. Lee, K. W. Leung, and E. K. N. Yung, "Technique for improving coupling between microstripline and dielectric resonator antenna," *Electron. Lett.*, vol. 35, no. 5, pp. 357–358, Mar. 1999.

[22] G. P. Junker, A. A. Kishk, A. W. Glisson, and D. Kajifez, "Effect of air gap on cylindrical dielectric resonator antenna operating in TM_{01} mode," *Electron. Lett.*, vol. 30, no. 2, pp. 97–98, Jan. 1994.

[23] G. P. Junker, A. A. Kishk, A. W. Glisson, and D. Kajfez, "Effect of fabrication imperfections for ground-plane-backed dielectric-resonator antennas," *IEEE Antennas Propag. Mag.*, vol. 37, no. 1, pp. 40–47, Feb. 1995.

[24] G. Drossos, Z. Wu, and L. E. Davis, "Aperture-coupled cylindrical dielectric resonator antenna," *Microw. Opt. Technol. Lett.*, vol. 20, no. 6, pp. 407–414, 1999.

[25] S. Fakhte, H. Oraizi, and R. Karimian, "A novel low-cost circularly polarized rotated stacked dielectric resonator antenna," *IEEE Antennas Wireless Propag. Lett.*, vol. 13, pp. 722–725, 2014.

[26] A. Petosa, N. Simons, R. Siushansian, A. Ittipiboon, and M. Cuhaci, "Design and analysis of multisegment dielectric resonator antennas," *IEEE Trans. Antennas Propag.*, vol. 48, no. 5, pp. 738–742, May 2000.

[27] S. Yarga, K. Sertel, and J. L. Volakis, "Multilayer dielectric resonator antenna operating at degenerate band edge modes," *IEEE Antennas Wireless Propag. Lett.*, vol. 8, pp. 287–290, 2009.

[28] M. Ranjbar Nikkhah, P. Loghmannia, J. Rashed-Mohassel, and A. A. Kishk, "Theory of ESPAR design with their implementation in large arrays," *IEEE Trans. Antennas Propag.*, vol. 62, no. 6, pp. 3359–3364, Jun. 2014.

[29] X. Fang, K. W. Leung, and E. H. Lim, "Singly-fed dual-band circularly polarized dielectric resonator antenna," *IEEE Antennas Wireless Propag. Lett.*, vol. 13, pp. 995–998, 2014.

[30] S. Dhar, K. Patra, R. Ghatak, B. Gupta, and D. R. Poddar, "A dielectric resonator-loaded minkowski fractal-shaped slot loop heptaband antenna," *IEEE Trans. Antennas Propag.*, vol. 63, no. 4, pp. 1521–1529, Apr. 2015.

[31] A. A. Abdulmajid, Y. Khalil, and S. Khamas, "Higher-order-mode circularly polarized two-layer rectangular dielectric resonator antenna," *IEEE Antennas Wireless Propag. Lett.*, vol. 17, no. 6, pp. 1114–1117, Jun. 2018.

[32] M. Yang, Y. Pan, and W. Yang, "A singly fed wideband circularly polarized dielectric resonator antenna," *IEEE Antennas Wireless Propag. Lett.*, vol. 17, no. 8, pp. 1515–1518, Aug. 2018.

[33] A. M. Faiz, N. Gogosh, S. A. Khan, and M. F. Shafique, "Effects of an ordinary adhesive material on radiation characteristics of a dielectric resonator antenna," *Microw. Opt. Technol. Lett.*, vol. 56, no. 6, pp. 1502–1506, 2014.

SAEED FAKHTE was born in Amlash, Iran, in 1987. He received the B.Sc. degree from the Sharif University of Technology, Tehran, Iran, in 2009, and the M.Sc. and Ph.D. degrees in electrical engineering from the Iran University of Science and Technology, Tehran, in 2012 and 2017, respectively. In 2016, he was a Visiting Ph.D. Student with the Politecnico di Torino, Torino, Italy. He is currently a Researcher with the Politecnico di Torino, where he is involved in the area of the antenna development for RF applications. He has authored or co-authored over 10 papers in peer-reviewed journals. His research interests include various areas of microwave and antenna engineering, such as dielectric resonator antennas, microstrip antennas, and microwave components. He served as a Reviewer for the IEEE Transactions on Antennas and Propagation, the IEEE Antennas and Wireless Propagation Letters, the *IET Microwaves, Antennas and Propagation*, the *IET Electronic Letters*, the *International Journal of RF and Microwave Computer-Aided Engineering*, and other journals on antennas and electromagnetics.

LADISLAU MATEKOVITS (M'94–SM'11) received the degree in electronic engineering from the Institutul Politehnic din Bucureşti, Romania, in 1992, and the Ph.D. degree in electronic engineering from the Politecnico di Torino, Italy, in 1995. Since 1995, he has been with the Electronics Department, Politecnico di Torino, where he became an Assistant Professor, in 2002, and an Associate Professor, in 2014. In 2009, he was a Marie Curie Fellow with Macquarie University, Sydney, NSW, Australia, for two years, where he is currently an Honorary Fellow. He has authored more than 320 publications in journals, conferences, workshops, and book chapters. His main research activities include computational electromagnetics, optimization techniques, and active and passive metamaterials. He has delivered seminars on these topics all around the world: Europe, USA, Australia, China, and Russia. He is a member of the Organizing Committee of the International Conference on Electromagnetics in Advanced Applications, and the technical program committees of several conferences. He was a recipient of various awards, including the 1998 URSI Young Scientist Award and the Best AP2000 Oral Paper on Antennas at the ESA-EUREL Millennium Conference on Antennas and Propagation. He was the Assistant Chairman and the Publication Chairman of the European Microwave Week 2002, Milan, Italy, and the General Chair of the BodyNets 2016, Torino, Italy. He serves as an Associate Editor for the IEEE Antennas and Wireless Propagation Letters, the IEEE Access, and the *IET Microwaves, Antennas and Propagations*, and as a reviewer for different journals.

IMAN ARYANIAN was born in Tehran, Iran, in 1986. He received the B.Sc. degree in electrical engineering and the M.Sc. and Ph.D. degrees in electrical communication engineering from the Amirkabir University of Technology, Tehran, Iran, in 2008, 2010, and 2016, respectively. He is currently an Assistant Professor with the Iran Telecommunication Research Center, Tehran. His research interests include the areas of the reflectarray antenna, computational electromagnetic, semiconductor RF modeling, electromagnetic theory, and computational electromagnetics.